THREE-DIMENSIONAL WEIGHT FUNCTION ANALYSES AND STRESS INTENSITY FACTORS FOR GENERAL SURFACE AND CORNER CRACK EMANINATING FROM CIRCULAR HOLE

W. Xu[1]*, B. Zhang[1] and X.R. Wu[2]

[1]School of Aeronautics and Astronautics, Shanghai Jiao Tong University, Shanghai 200240, China
[2]AECC Beijing Institute of Aeronautical Material, Beijing 100095, China
* Corresponding author: xuwu@sjtu.edu.cn

ABSTRACT

Comprehensive study of aircraft structural failures showed that the most prevalent failure is due to cracks originating from fastener holes, where stress concentration takes place. Stress intensity factors (SIFs) for these crack configurations are the prerequisite for evaluation of the critical crack sizes and fatigue lives of components during which the initial cracks would grow to the critical size. The computational efficiency for SIF is critical, since for every crack growth step, the crack size changes and so are the SIFs. Much work has been done to obtain SIFs of a single and double symmetric 3D cracks at riveted holes subjected to typical loadings. However, due to the complexity of the problem, limited work has been done for the SIFs of more general and complex case, eccentric and asymmetric surface and corner cracks, and combination of surface and corner cracks subjected to arbitrary load cases. These crack configurations are very common, but are too complicated to be analytically tackled. The SIF solution is still highly demanded for the damage tolerance analyses of various flaws at fastener hole. In this paper, the 3D slice synthesis weight function method (SSWFM) is further developed to calculate the 3D SIFs for such general and complex case. The resulting 3D SIFs are extensively compared to those obtained from FEM/Franc3D; very good agreement is achieved. However, the developed SSWFM is about 450 times faster than FEM/Franc3D in calculation of the 3D SIFs for the present complex crack geometry. It can be used to obtain 3D SIFs of most of the surface and surface-corner crack configurations from a hole in practical engineering, and would be useful for 3D fatigue crack growth analysis of rivet joint structures subjected to various load cases.

Keywords: Weight function method, hole-edge crack, asymmetric and eccentric cracks, slice synthesis method, stress intensity factor

1. INTRODUCTION

The majority of aircraft structural failures are attributed to fatigue crack initiation and propagation from riveted joints [1-2]. The fatigue life spent by the growth of small three-dimensional (3D) cracks is very important for damage tolerance design. To predict fatigue crack growth life, commercial tools such as NASGRO [3] and AFGROW [4] have been developed and widely used in aerospace industry. Fatigue crack growth lives of a single and double symmetric 2D and 3D cracks at riveted holes subjected to typical loadings can be predicted by using these tools. However, it is difficult to deal with the asymmetric and eccentric 3D crack cases at riveted holes as shown in Fig.1. This is because stress intensity factors (SIFs) for two asymmetrical corner cracks, asymmetrical surface cracks, and also surface-corner cracks combination, are rarely available. The complexity of these crack configurations makes their SIF-solutions virtually intractable by analytical methods. Therefore, accurate and efficient methods of SIF-determination for engineering structures with complicated 3D crack geometries under various load cases are still highly desirable.

There are very limited pure analytical SIF-solutions for 3D cracks, except for the case of an elliptical crack embedded in an infinite elastic solid. For complicated practical 3D crack problems, various numerical methods are often used, such as boundary element method [5], boundary integral equation method [6], finite element method (FEM) [7-9] and the X-FEM [10,11]. The well-known Newman-Raju [12-13] SIF-equations for a single and double symmetrical corner/surface crack at a circular hole were obtained by conducting a large amount of finite element analyses, and the Fawaz-Andersson *p*-version FE solutions using 100000-140000 degrees of freedom [14]. Grandt [15] obtained the SIFs of single surface crack under remote tension and crack face pressure using finite element alternating method (FEAM). To capture the stress singularity at the crack tip, singular elements were developed and have been widely used to improve SIF-accuracy [16]. With the classical FEM, very fine mesh is required to model the crack tip, which makes it hard and tedious to mesh 3D crack geometries. To alleviate such difficulty, special 3D crack mesh generators, for example Franc3D [17] were developed to automatically mesh the crack and post-processing the stress-strain-displacement field to obtain SIFs. For fatigue crack growth analysis, continuous re-meshing the cracked body for each crack size increment is required, which is very time-consuming. The X-FEM was originally proposed to overcome the requirement for re-meshing for modeling crack growth. Recent development of this method for modeling 3D crack growth can be found in [10,11].

As pointed out by McClung et al. [18], it is costly and impractical to use FEM for 3D fatigue crack growth analysis, for which hundreds and thousands of SIFs are need for different crack lengths and various load cases encountered in service. The weight function method (WFM) is powerful for calculating SIFs under arbitrary loading cases [18-29]. It has been widely used to calculate the SIFs since the early 1970s [19-20]. Recent reviews of the progress were given by Wu and Xu [22-24]. WFMs for through-thickness (2D) crack is now well developed, various weight functions are available in Refs. [21, 23, 29]. However, development and widespread engineering applications of WFMs for 3D crack problems is still an important research area. The point weight function methods (PWFMs) were developed by Orynyak et al. [27], and Wang and Glinka [28]. By introducing a fictitious symmetrical load, it was modified for semi-elliptical surface cracks in finite thickness plate with different aspect ratio of cracks by Jin et al. [30], Ghajar and Googarchin [31]. Recently, Guo et al. [32] obtained SIFs of quarter-elliptical single corner crack emanating from a circular hole by using this method. The PWFM for general 3D crack requires known reference SIFs under certain reference load cases by using 3D FE analysis, to determine the coefficients in the 3D crack-geometry-specific weight function. It is time-consuming to obtain a large amount of reference SIFs by FE analyses of the present asymmetrical surface and corner cracks, since there are six geometric variables (a_l, a_r, c_l, c_r, r, t) involved. Therefore, more efficient method is highly desirable.

A slice synthesis weight function method (SSWFM), was developed by Zhao-Wu-Yan [33-34]. The method is based on a combination of the slice-synthesis technique that was first proposed by Fujimoto [35] and further developed and improved by Zhao et al. [33-34,36-39], and the 2D analytical WFM by Wu and Carlsson [21,40]. The basic idea of the SSWFM is to decompose the 3D crack model into two orthogonal slices with interaction shear stresses. The two orthogonal slices can be analyzed by using available 2D analytical weight functions [21,23]. This method has very high computational efficiency and no reference 3D-SIFs are needed, which is very advantageous for dealing with arbitrary 3D crack configurations. The SSWFM has been used to analyze a variety of 3D crack configurations, including a single and symmetric double corner and surface crack emanating at a circular hole and notch [34,36-39,41-42]. Bakuckas [43] made a comparison of 3D SIFs for two symmetric corner cracks in a straight-shank hole, obtained by various numerical methods (including Franc3D, FEAM, DIM, FADD3D and GIL) and also the SSWFM, and concluded that SIFs from the SSWFM were within a narrow band of 3% about the average solution. Recently, closed form 2D weight functions of two unequal-length hole-edge cracks and eccentric crack were derived by Zhang et al. [44-46]. It was used as a basic slice to calculate SIFs of asymmetric double corner cracks at a circular hole by an improved SSWFM. Extensive comparisons to the literature data and numerical results by using FEM have shown that the SIFs obtained by using SSWFM are of high accuracy.

In this paper, the improved SSWFM is further utilized to determine 3D SIFs for three types of new 3D crack geometries: two asymmetric corner cracks, two asymmetric surface cracks and combination of surface-corner cracks at a circular hole in an infinite plate subjected to two typical load cases. The obtained 3D SIFs are verified by comparing to results from extensive FEM analysis. Solution accuracy of the improved SSWFM is confirmed.

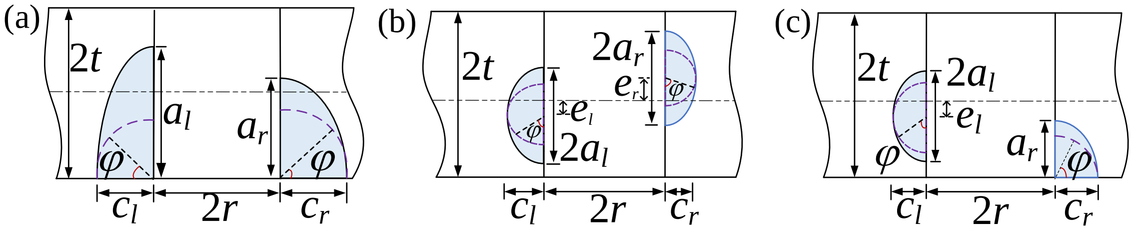

Fig.1 General Surface and corner cracks at a cicular hole; (a) asymmetric corner cracks; (b) asymmetric and eccentric surface corner cracks; and (c) combination of surface and corner cracks.

2. 3D SSWFM FOR ASYMMETRICAL CORNER, SURFACE AND SURFACE-CORNER CRACKS

The concept of SSWFM is to decompose the 3D crack problem into basic slice and spring slice of infinitesimal thickness [33,34]. Interaction between the slice-set is represented by the spring stress $S(x,y)$. 2D weight functions of these slices are used to calculate the crack opening displacement (COD) and further to determine the spring stress $S(x,y)$. Once $S(x,y)$ is obtained, the SIFs for each slices are computed using 2D WFM and used to compound the corresponding 3D SIFs at any point along the crack front. For the present asymmetric and eccentric hole-edge cracks shown in Fig.1, their slice-sets are different, and will be introduced in Sections 2.1-2.3, respectively.

2.1 Two asymmetrical corner cracks

A 3D crack configuration with asymmetric corner cracks originating from a circular hole is shown in Fig.2.

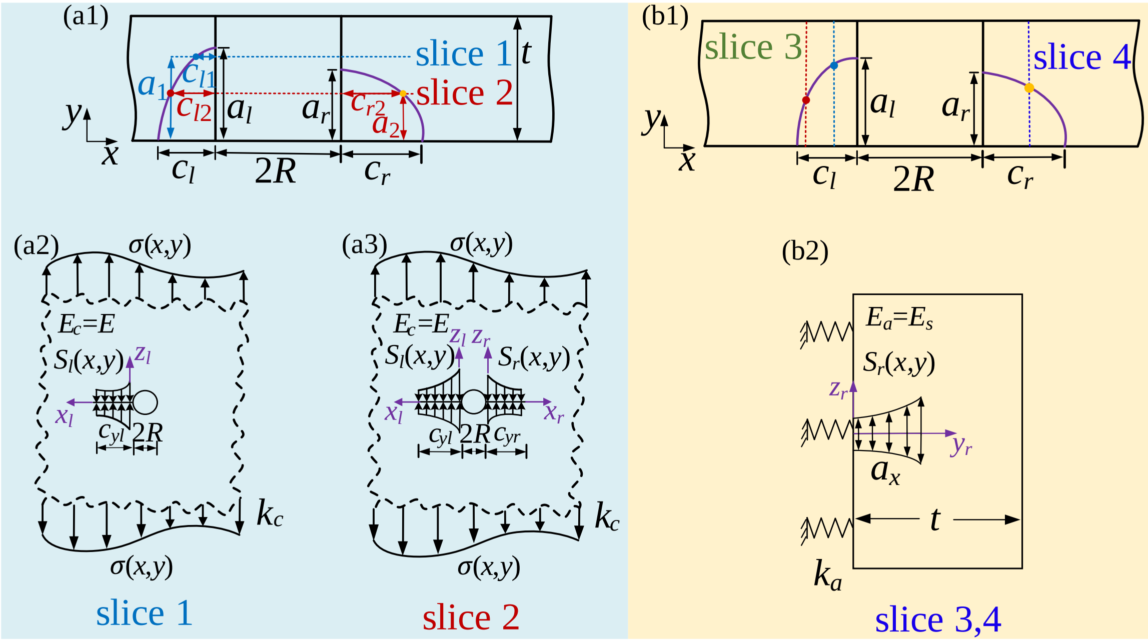

Fig.2. Slice model for two asymmetric corner cracks at a hole: (a) basic slice (hole-edge cracks); (b) spring slice (edge crack in a finite width sheet with lateral edges constrained).

According to Zhao et at. [33], the 3D SIF at a given parametric angle φ, $K(\varphi)$, is

$$K_j(\varphi)=\frac{1}{1-\eta^2}\left\{K_{cj}^4\left(c_{yl},c_{yr}\right)+\left[\frac{E_j}{E_{sj}}K_{aj}\left(a_{xj}\right)\right]^4\right\}^{1/4}\left(-1\right)^n,\ j=l,\ r \tag{1a}$$

$$E_{s_j}=E_j\left(\frac{\Phi_j}{1-\nu^2}-1\right)\frac{c_j}{a_j},\ a_j/c_j\le 1;\quad E_{s_j}=E_j\left(\frac{\Phi_j}{1-\nu^2}-\frac{c_j}{a_j}\right),\ a_j/c_j>1,\ j=l,\ r \tag{1b}$$

$$\Phi_j=\left[1.0+1.464\left(a_j/c_j\right)^{1.65}\right]^{1/2},\ a_j/c_j\le 1;\quad \Phi_j=\left[1.0+1.464\left(c_j/a_j\right)^{1.65}\right]^{1/2},\ a_j/c_j>1 \tag{1c}$$

where φ is the parametric angle at a point along the crack front as shown in Fig. 1. The subscript 'j' represents left or right crack of the hole. E and E_s are Young's modulus of the basic slice and spring slice, c_y and a_x are crack length of basic slice and spring slice, respectively. η=0 for free surface and $\eta=\nu$ for points inside the body. n=2 for K_i>0 ($i=a$, c), otherwise n=1. K_c and K_a are SIFs of the basic and spring slices, which can be obtained by the 2D WFM Eqs.(2a) and (2b), respectively.

$$\begin{aligned}K_{cj}(c_{yl},c_{yr})&=\int_0^{c_{yl}}\left[\sigma_l\left(x,y\right)-S_l\left(x,y\right)\right]\cdot m_{cj}\left(c_{yl},c_{yr},r,x\right)\mathrm{d}x\\&+\int_0^{c_{yr}}\left[\sigma_r\left(x,y\right)-S_r\left(x,y\right)\right]\cdot m_{cj}\left(c_{yl},c_{yr},r,x\right)\mathrm{d}x\end{aligned} \tag{2a}$$

$$K_{aj}(a_{xj})=\int_0^{a_{xj}}S_j\left(x,y\right)m_a\left(a_{xj}/t,y/t\right)\mathrm{d}y \tag{2b}$$

where $\sigma_l(x,y)$ and $\sigma_r(x,y)$ is the stress distribution at the crack location in the un-cracked body subjected to external load. m_c is the 2D weight function of a single hole-edge crack (see slice 1 in Fig.2) or two unequal-length hole-edge cracks in an infinite sheet (see slice 2 in Fig.2). The former is available in [21], while the latter is derived by the present writer in [44]. m_a is weight function of the edge crack in the spring slice dependent with boundary constraint k_a. It is between the weight functions of a single edge crack m_{se} and double symmetrical collinear edge cracks m_{de} in a finite plate corresponds to k_a=0 and $k_a=\infty$, respectively [21]. With the weight functions for these two limiting conditions, the 2D weight functions for the spring slice is determined by Eq.(3) in the original SSWFM.

$$m_a=m_{de}+T(k_a)(m_{se}-m_{de}) \tag{3}$$

where, the transition factor $T(k_a)$ varies between zero and unity, representing the transition from the fixed boundary condition to the free boundary condition [33]. For the present case of infinite plate, $T(k_a)$ is zero according to Zhao et al. [33].

The spring force $S(x, y)$ in Eq.(2) represents the interaction between the slices. It can be determined by the displacement compatibility condition, i.e., the displacements from the basic and spring slices at a point on the 3D crack surface should be identical. Using the 2D WFM, the CODs for the two sets of slices can be determined by

$$U_{aj}(a_{xj}, y) = \frac{1}{E_{aj}} \int_y^{a_{xj}} K_{aj}(\xi) \cdot m_a(\xi/t, y/t) \mathrm{d}\xi \tag{4a}$$

$$U_{cl}(c_{yl}, c_{yr}, x) = \frac{1}{E_{cl}} \int_x^{c_{yl}} K_{cl}(\xi, c_{yr}) \cdot m_{cl}(\xi, c_{yr}, r, x) \mathrm{d}\xi \tag{4b}$$

$$U_{cr}(c_{yl}, c_{yr}, x) = \frac{1}{E_{cr}} \int_x^{c_{yr}} K_{cr}(c_{yl}, \xi) \cdot m_{cr}(c_{yl}, \xi, r, x) \mathrm{d}\xi \tag{4c}$$

According to the displacement compatibility $U_{aj}=U_{cj}$, the governing equation for the spring force $S_l(x,y)$ and $S_r(x,y)$ is given by

$$\begin{aligned} &\int_x^{c_{yl}} \int_0^{\xi} \left[\sigma_l(x, y) - S_l(x, y)\right] \cdot m_{cl}(\xi, c_{yr}, r, x) \mathrm{d}x \cdot m_{cl}(\xi, c_{yr}, r, x) \mathrm{d}\xi \\ &= \frac{E_l}{E_{sl}} \int_y^{a_{xl}} \int_0^{\xi} S_l(x, y) \cdot m_a(\xi/t, y/t) \mathrm{d}y \cdot m_a(\xi/t, y/t) \mathrm{d}\xi \end{aligned} \tag{5a}$$

$$\begin{aligned} &\int_x^{c_{yr}} \int_0^{\xi} \left[\sigma_r(x, y) - S_r(x, y)\right] \cdot m_{cr}(c_{yl}, \xi, r, x) \mathrm{d}x \cdot m_{cr}(c_{yl}, \xi, r, x) \mathrm{d}\xi \\ &= \frac{E_r}{E_{sr}} \int_y^{a_{xr}} \int_0^{\xi} S_r(x, y) \cdot m_a(\xi/t, y/t) \mathrm{d}y \cdot m_a(\xi/t, y/t) \mathrm{d}\xi \end{aligned} \tag{5b}$$

Once $S_l(x,y)$ and $S_r(x,y)$ are determined by solving Eq.(5), the SIFs for the 3D crack can be obtained by Eqs. (1-2), subsequently. It is noteworthy that for large cracks (i.e. long and deep with $c/r>1.0$, $a/t>0.6$), $T(k_a)=0$ is over constrained, and it may affect the solution accuracy. Furthermore, it is also noted that the solution accuracy tends to decline for deep cracks (larger a/t). To overcome this problem, an effective but simple technique is proposed herein. Both the weight functions for a single edge crack (free of constrain, $T(k_a)=1$) and double symmetrical collinear edge cracks (fixed, $T(k_a)=0$) are used for m_a in Eqs.(2b) and (4a) and (5) to calculate the SIFs separately, giving to two sets of SIFs for the two limiting conditions: $K_{T(k_a)=0}$ and $K_{T(k_a)=1}$. By taking the average of the two sets of SIFs, the resulting K becomes

$$K = \left(K_{T(k_a)=0} + K_{T(k_a)=1}\right)/2 \tag{6}$$

2.2 Eccentric and asymmetric surface cracks

A 3D crack configuration with two eccentric and asymmetric semi-elliptical surface cracks with different eccentricity e_l/t, e_r/t originating from a circular hole is shown in Fig.1(b). The cracked body is divided into two series of orthogonal slices of infinitesimal thickness in the *xz* and *yz* planes. The mechanical coupling between these slices is represented by the spring stress $S(x,y)$. For an interested point on the crack front, the basic slice and corresponding spring slice are shown in Fig.3. The basic slice shown in Fig.3(a) is either a single or two hole-edge cracks in an infinite sheet subjected to external load and spring stress $S(x,y)$. While, the spring slice is an eccentrical crack in a finite width sheet subjected to $S(x,y)$ only as shown in Fig.3(b). The lateral edges are constrained to simulate the effect of the restraint due to the uncracked body outside the region occupied by the spring slice.

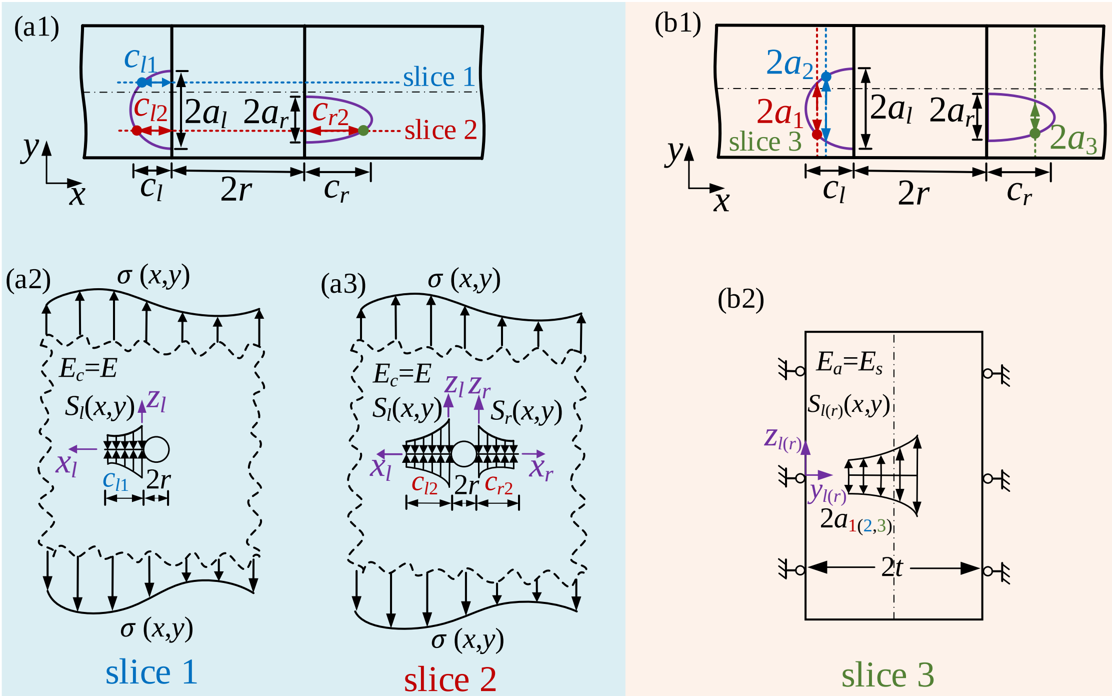

Fig.3. Slice model for two eccentric surface cracks at a hole: (a) basic slice (hole-edge cracks); (b) spring slice (eccentric crack in a finite width sheet with lateral edges constrained).

The SSWFM introduced in Section 2.1 can also be applied to calculate the 3D SIFs of the asymmetric surface cracks as shown in Fig.1(b). The difference is that, a constrained eccentric crack in a finite sheet, is used to model the surface crack [46], the weight function for an eccentric crack in a finite width sheet with constrained edges shown in Fig.3b is derived by the present writer [46].

For the present eccentric surface crack, a large number of discrete points (63 points) on each crack surface shown in Fig.4 are used to determine the coefficients χ_n and χ_k. The normalized coordinates were given in [46]. Substituting the location (x, y) into Eq.(5), 126 displacement compatibility equations will be obtained. The coefficients χ_n (n=1~14) and χ_k (k=1~14) of $S_l(x,y)$ and $S_r(x,y)$ for both crack surfaces can be solved by using the least square method. Subsequently, the 3D SIFs are determined by Eqs.(1,2,5).

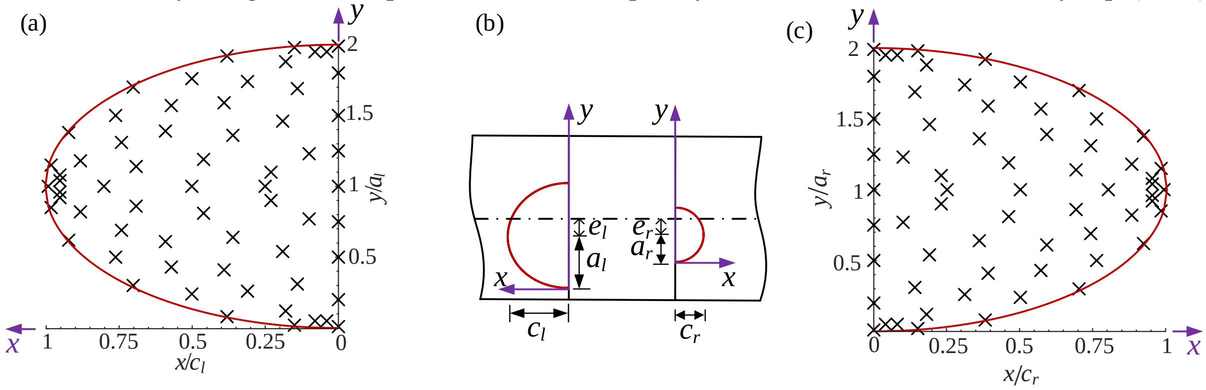

Fig.4. COD-compatibility points on surface crack: (a) left surface crack; (b) coordinate systems of hole-edge surface crack; (c) right surface crack.

2.3 Eccentric surface and corner cracks

For the 3D SIFs of the combination of an eccentrical semi-elliptical surface crack and a quarter-elliptical corner crack as shown in Fig.1(c). The only difference is that one more type of spring slice, a constrained edge crack in a finite sheet, is used to model the corner crack [45,46]. The construction of the basic and spring slice-sets is shown in Fig.5. The weight function of the constrained edge crack shown in Fig.5(b) can be approximated either by the weight function of an edge crack m_{se} or by that of double edge cracks m_{de}, which are available in Refs. [21].

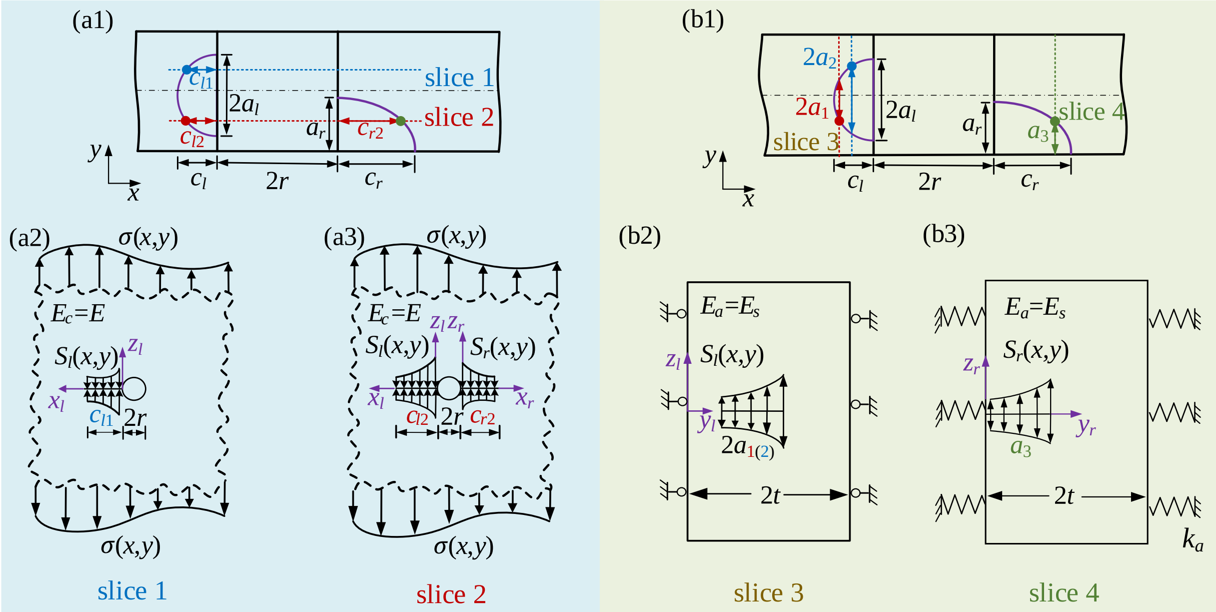

Fig.5. Slice model for surface/corner cracks at a hole: (a) basic slice (unequal-length hole-edge cracks); (b) spring slice (eccentric crack with constrained edges; edge cracks with elastic constraint).

3. APPLICATION AND VERIFICATION OF SSWFM

The non-dimensional SIF of the corner cracks is defined by

$$f = \frac{K \cdot \Phi}{S_i \sqrt{\pi a}} \tag{7}$$

where, K is the SIF of from Eq. (1), a is the crack depth, S_i is the stress induced by applied load. The subscript i (i=t, b and w) represents the load type, S_t=S for remote tension, S_b=$3M/Wt^2$ for out of plane bending, S_w=$P/(2rt)$ for wedge loading, where P is the total applied force (unit thickness) in z-direction over the arc from θ=0 to π, and σ_n=$3P/(4rt)\cdot\cos^2(\theta)$ refer to [12] in Fig. 6c. The SIFs determined by using SSWFM will be verified by the results from FEM.

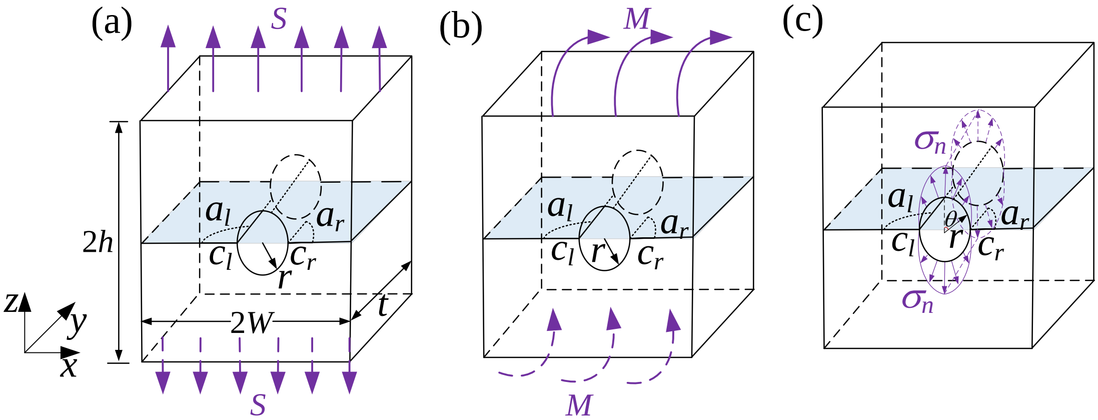

Fig. 6 Asymmetric corner crack configuration subjected to three typical loads: (a) remote tension; (b) out of plane bending; (c) wedge loading.

3.1 3D finite element model

To obtain highly accurate SIFs, special software Franc3D [17] is used to mesh the corner cracks. A typical FE model is shown in Fig.7, where very fine collapsed quarter-point singular elements around crack front are used to characterize the stress singularity. The 20-noded hexahedral elements are adopted elsewhere. The total number of elements is about 95,000. The FE model generated by Franc3D is then submitted to ABAQUS/Standard to solve the displacement/strain/stress fields, which will be post-processed by Franc3D to determine SIFs using M-integral [47].

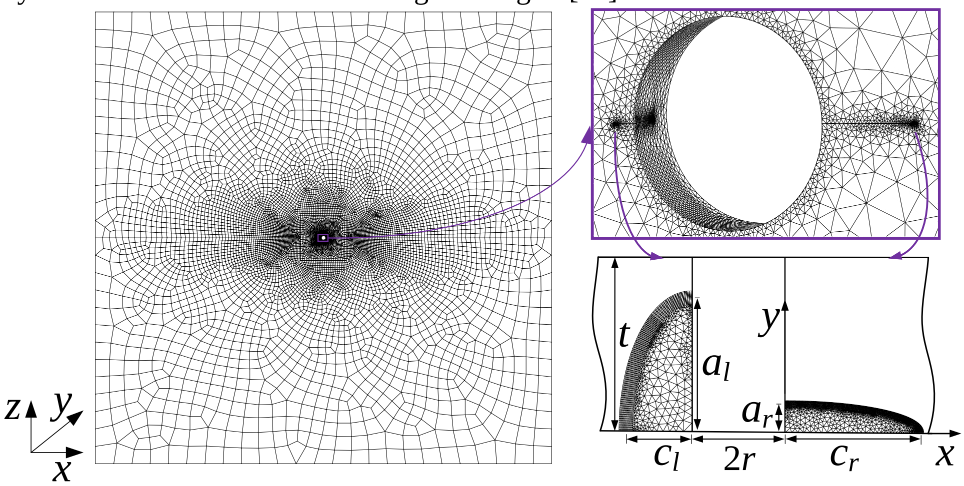

Fig. 7 Typical FE mesh for two corner cracks modeled by using Franc3D.

3.2 3D SIFs for asymmetric corner cracks

The SIFs for two asymmetric cracks subjected to three typical load cases shown in Fig.10 are calculated by using the present SSWFM analysis. Results for three typical crack configurations under remote tension are shown in Fig.8a-d. In Fig.8a-c, the SIFs for both crack fronts are provided. Only the SIFs for the small crack is given in Fig.8d. Also shown in these figures are the results from Franc3D. The differences are mostly within 5%. For some cases, the differences in a small region near the plate surface (φ=0) is somewhat larger (Fig. 8c). To show the interactions between the corner cracks, the SIFs of a single corner crack are compared in Fig.8d. The influence of the large corner cracks on the SIF of the small crack is obvious as shown in Fig. 8d. It cannot be neglected for fatigue crack growth prediction, since most of the fatigue life is consumed in the small crack growth stage. Therefore, the present SSWFM can improve the accuracy of fatigue crack growth life prediction for two asymmetric hole-edge corner cracks.

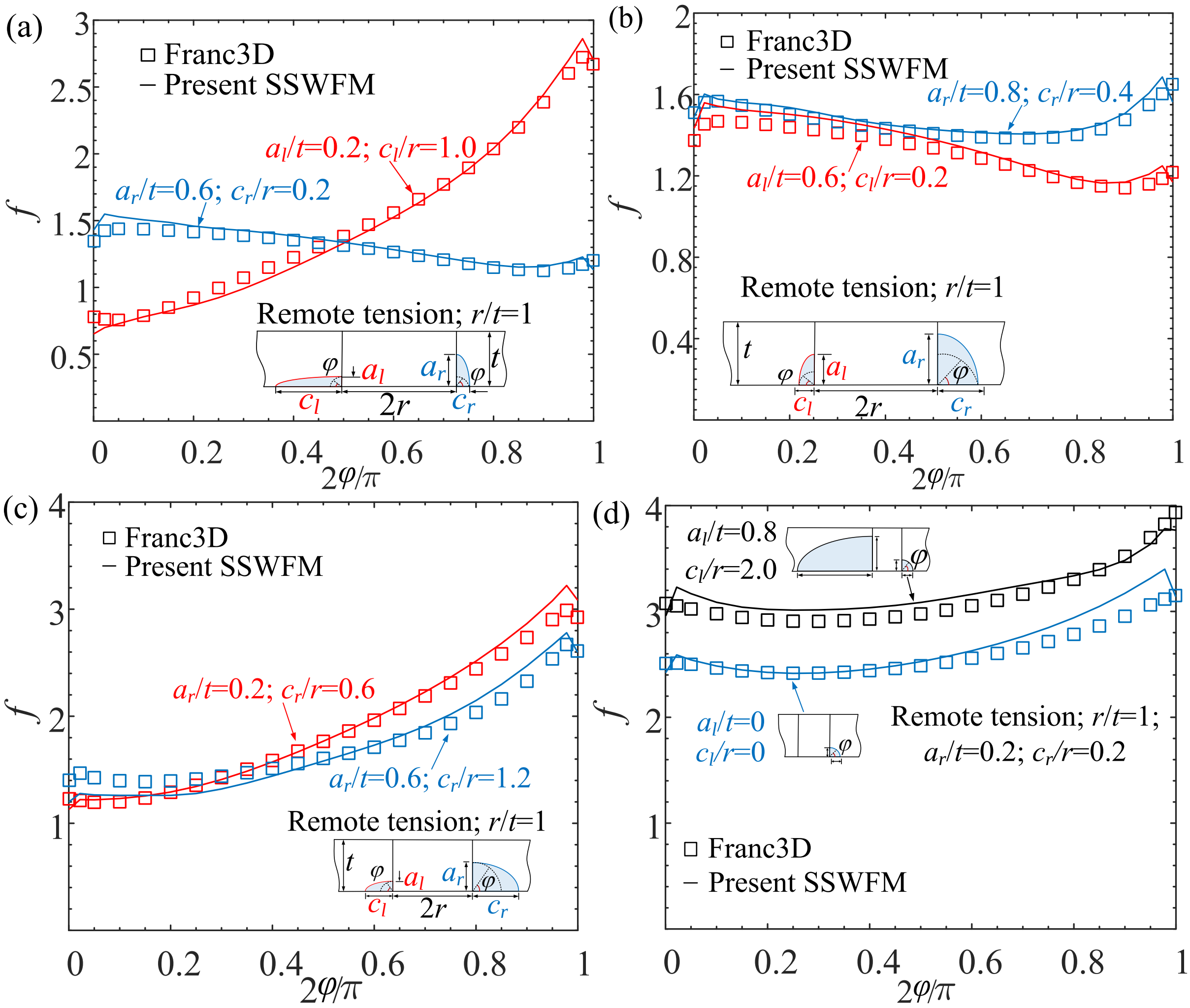

Fig. 8 SIFs of two asymmetrical corner cracks at a hole under remote tension (r/t=1): (a) a_l/t=0.2; c_l/r=1.0; a_r/t=0.6; c_r/r=0.2; (b) a_l/t=0.6; c_l/r=0.2; a_r/t=0.8; c_r/r=0.4; (c) a_l/t=0.2; c_l/r=0.6; a_r/t=0.6; c_r/r=1.2; (d) effect of the large corner crack on the SIF of the small crack.

3.3 3D SIFs for asymmetric and eccentric surface cracks

The SIFs for two eccentric and asymmetric surface cracks subjected to the three typical load cases are calculated by using the present SSWFM. For remote tension, the SIFs for four quite different crack configurations with different combination of crack size and eccentricity are shown in Fig.9(a-d) represented by the solid (left crack) and dashed (right crack) lines. For comparison, FE analysis are conducted, the corresponding SIFs are also shown in Fig.9 denoted by the square symbols. It is observed that the SIFs obtained from SSWFM and FEM/Franc3D are in good agreement. The relative difference is within 8% for most cases, the local maximum is less than 13%. SSWFM is a simplified model to decompose the complex 3D crack problem into a superposition of two 2D crack problems. The well-known boundary layer effect would also affect the accuracy of the SIFs near free surface. The difference between the present SSWFM and Franc3D may be due to the assumption of SSWFM and the boundary layer effect discussed in the previous literature [34].

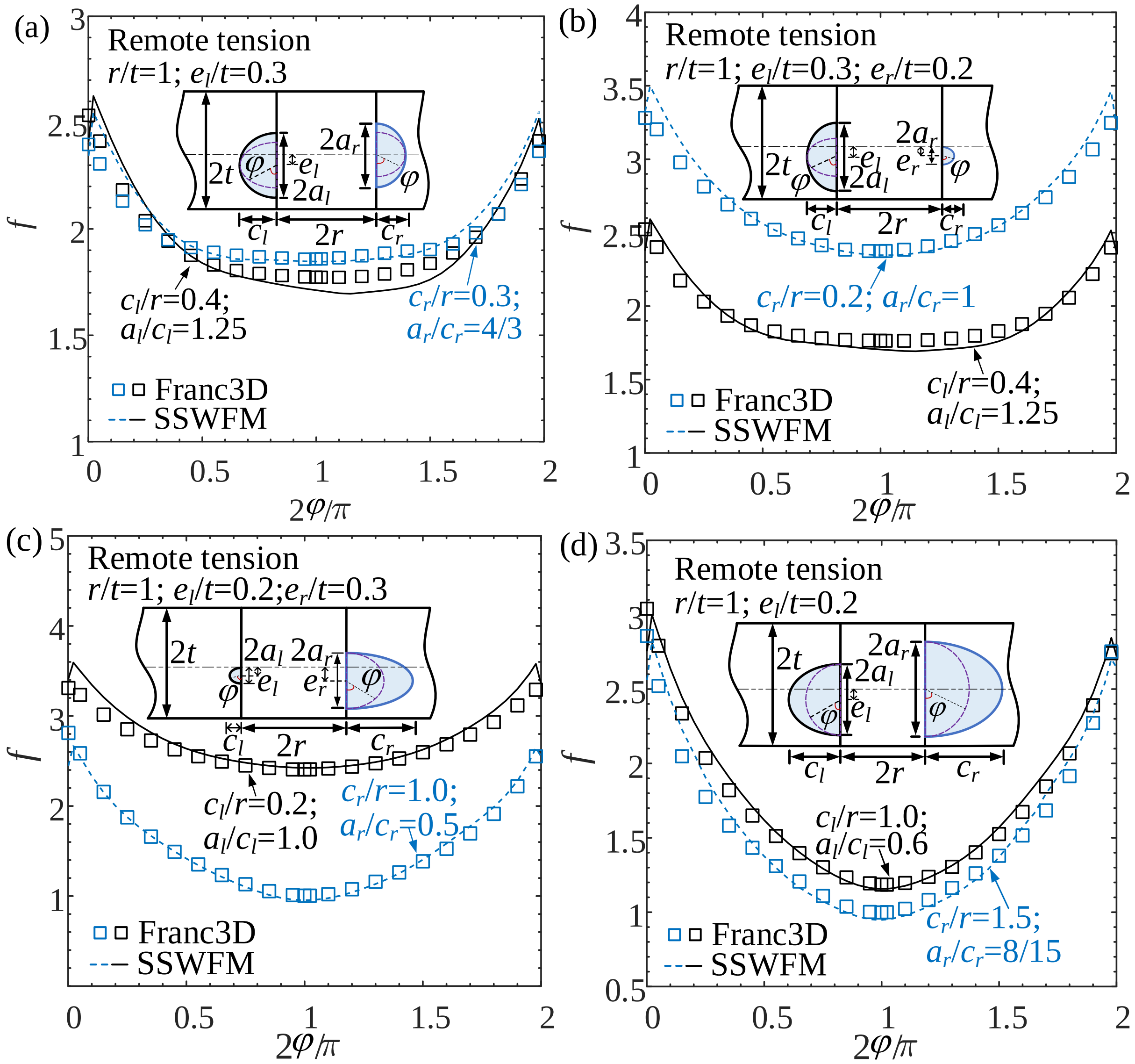

Fig.9. SIFs of two eccentric and asymmetric surface cracks under remote tension (r/t=1): (a) c_l/r=0.4, a_l/c_l=1.25, e_l/t=0.3, c_r/r=0.3, a_r/c_r=4/3; (b) c_l/r=0.4, $a_l/\ c_l$ =1.25, e_l/t=0.3, c_r/r=0.2, a_r/c_r=1, e_r/t=0.2; (c) c_l/r=0.2, a_l/c_l=1, e_l/t=0.2, c_r/r=1.0, a_r/c_r=0.5, e_r/t=0.3; (d) c_l/r =1.0, a_l/c_l=0.6, e_l/t=0.2, c_r/r=1.5, a_r/c_r=8/15.

3.4 3D SIFs for corner-surface cracks

A combination of a surface-corner crack is a common crack configuration. The SIFs for different surface-corner cracks subjected to the three typical load cases are calculated by the present SSWFM. For the remote tension, the SIFs of the surface and corner cracks obtained from SSWFM are denoted by the solid and dashed lines, respectively, in Fig.10. For comparison, also shown in Fig.10 are the results from FEM/Franc3D represented by the square symbol. For the surface crack, the SIFs obtained from SSWFM and FEM/Franc3D are in good agreement, the relative difference is within 6% for most cases. The differences are somewhat larger near the plate surface (φ=0), with the maximum of 17% for the combination of big surface and corner cracks shown in Fig.10(d). For the corner crack, the relative difference of the SIFs obtained from SSWFM and FEM/Franc3D is generally less than 8%.

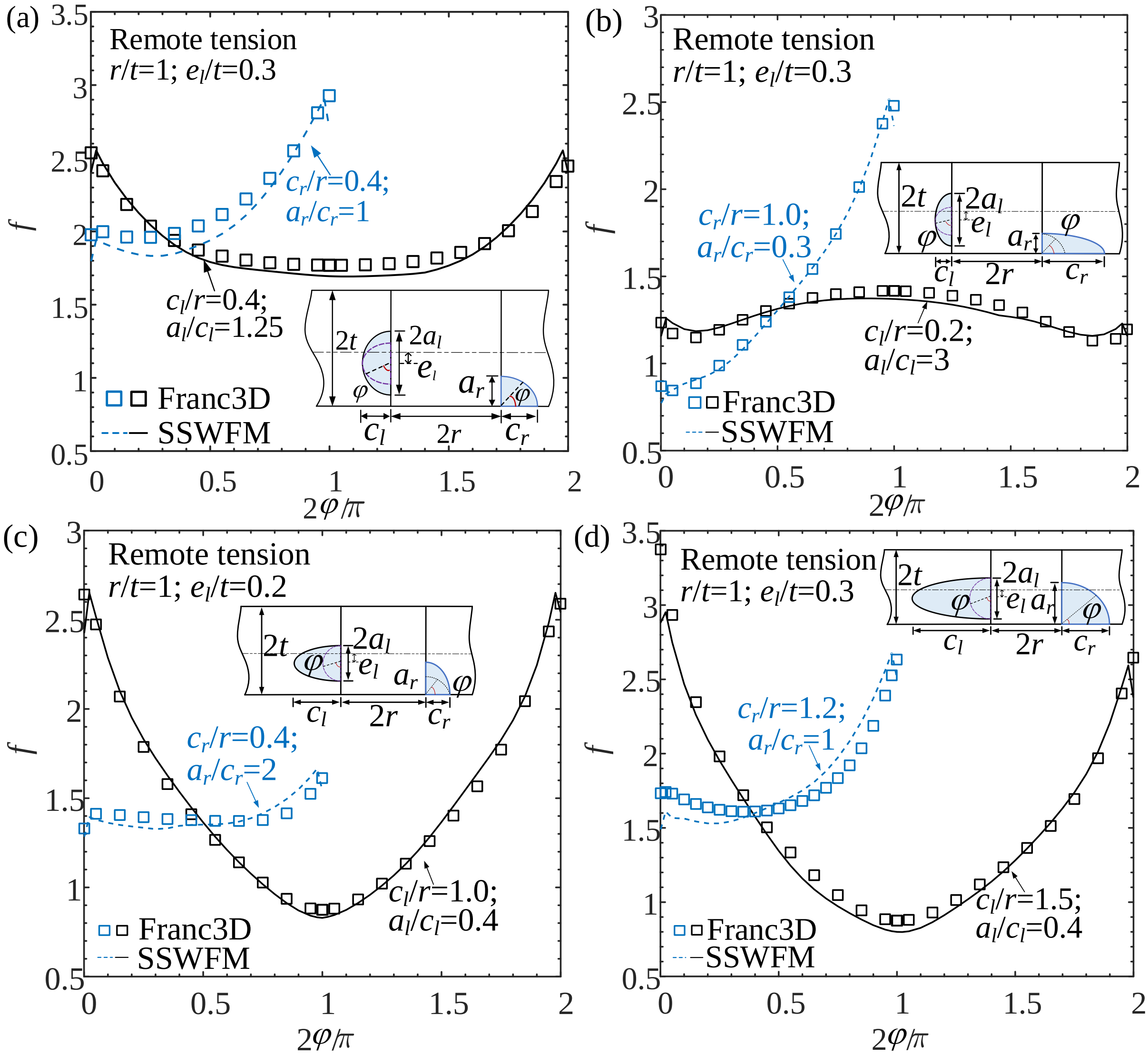

Fig.10. SIFs of surface-corner cracks under remote tension (r/t=1): (a) c_l/r =0.4,a_l/c_l=1.25, e_l/t=0.3, c_r/r=0.4, a_r/c_r=1; (b) c_l/r=0.2, a_l/c_l=3, e_l/t=0.3, c_r/r=1, a_r/c_r=0.3; (c) c_l/r=1, a_l/c_l=0.4, e_l/t=0.2, c_r/r=0.4, a_r/c_r=2; (d) c_l/r=1.5, a_l/c_l=0.4, e_l/t=0.3, c_r/r=1.2, a_r/c_r=1.

4. DISCUSSIONS

For every fatigue crack growth step, the crack geometry will be changed and so are the SIFs. A very large amount of SIFs are needed to predict the fatigue crack growth lives from a small 3D crack to the critical crack size. Therefore, computational efficiency for 3D SIFs is of crucial importance. FEM is very powerful for calculation of 3D SIFs of complex crack geometries. However, since the 3D crack size is usually small and there is a high stress gradient at the crack tip, it is very cumbersome to mesh a 3D cracked body. To alleviate this difficulty, professional software, such as Franc3D, has been developed to mesh the crack and to abstract the stress/strain/displacement field to calculate the SIF. With the help of the advanced software, high quality finite element model can be obtained. In addition, the modeling time is significantly reduced. Even so, it takes about 25 minutes to create the finite element model shown in Fig.9 by using Franc3D, and 5 minutes to complete the analysis by ABAQUS/Standard, respectively (PC: Intel(R) Core (TM) i7-8700 CPU @ 3.20GHz). In contrast, it needs merely about 4 seconds to calculate the SIFs of the surface cracks or surface-corner cracks by using the present SSWFM. This means that, the present SSWFM is about 450 times faster than FEM/Franc3D in calculation of 3D SIFs.

The PWFMs are alternative methods for calculation of the 3D SIF [30-32]. In the determination of the PWF, a large amount of reference 3D SIFs for the crack configuration are need to calibrate the correction coefficients in the PWF-expression. FEM is usually used to obtain the reference 3D SIFs. For the present eccentric and asymmetric surface cracks, there are too many geometry variables involved, which requires huge computational resource and therefore becomes impractical. However, for the present SSWFM, no reference 3D SIF-solutions are needed, only 2D weight functions are required, which are available for most common through-thickness crack configurations or can be easily derived by using the displacement-based WFM in Refs. [21]. In general, the results by the present SSWFM have good agreement with FEM/Franc3D, the difference of the two methods are mostly within 8%. Therefore, the present SSWFM is superior to PWFMs for the present eccentric and asymmetric hole-edge surface/corner cracks.

5. CONCLUSIONS

The weight function of complex 2D crack configuration was derived by the present author, with the present 2D weight functions, the SSWFM for two asymmetric corner cracks, surface cracks and corner-surface crack at a hole is established. SIFs for asymmetric corner cracks, surface cracks and corner-surface cracks at a hole under typical loading are determined using the present SSWFM. The obtained SIFs agree well with those from FE analysis based on Franc3D, most of the differences are less than 10%.

The present SSWFM is much more efficient than PWFM and FEM in calculation of the SIFs of asymmetric cracks at a hole. It is about 500 times faster than Franc3D in calculation of SIFs, and therefore will significantly enhance fatigue crack growth analysis capability for engineering structures with circular hole.

REFERENCES

[1] T. Swift, Damage tolerance capability, Int. J. Fatigue. 16(1) (1994) 75-96.
[2] J. Schijve, Multiple-site-damage fatigue of riveted joints. International Workshop on Structural Integrity of Aging Airplanes 1992; 1.
[3] NASGRO. Fracture mechanics and fatigue crack growth analysis software, Version 7.0. NASA Johnson Space Center and Southwest Research Institute, 2012.
[4] J. Harter, AFGROW users guide and technical manual. AFRL-VA-WP-TR-2008-XXXX, Air Force Research Laboratory; July 2008.
[5] DT. D. Nguyen, F. Javidan, M. Attar, S. Natarajan, Z. Yang, E.H. Ooi, E.T. Ooi, Fracture analysis of cracked magneto-electro-elastic functionally graded materials using scaled boundary finite element method, Theor. Appl. Fract. Mech. 118 (2022), 103228.
[6] W. Yi, Q.H. Rao, S. Luo, Q.Q. Shen, Z. Li, A new integral equation method for calculating interacting stress intensity factor of multiple crack-hole problem, Theor. Appl. Fract. Mech. 107 (2020), 102535.
[7] X. Zhao, Z.L. Mo, Z.Y. Guo, J. Li, A modified three-dimensional virtual crack closure technique for calculating stress intensity factors with arbitrarily shaped finite element mesh arrangements across the crack front, Theor. Appl. Fract. Mech. 109 (2020), 102695.
[8] Tabaza, O.H. Okada, Y. Yusa, A new approach of the interaction integral method with correction terms for cracks in three-dimensional functionally graded materials using the tetrahedral finite element, Theor. Appl. Fract. Mech. 115 (2021), 103065.
[9] X.F. Hu, W.H. Chen, P. Zhang, QC.T. Bui, W.A. Yao, A new crack-tip singular element for cracks in three-dimensional elastic bodies, Engng. Fract. Mech, 235 (2020), 107148.
[10] R. Verma, P. Kumar, R. Jayaganthan, H. Pathak, Extended finite element simulation on Tensile, fracture toughness and fatigue crack growth behavior of additively manufactured Ti6Al4V alloy, Theor. Appl. Fract. Mech. 117 (2022), 103163.
[11] F. Shi, D. Wang, Q. Yang, An XFEM-based numerical strategy to model three-dimensional fracture propagation regarding crack front segmentation, Theor Appl Fract Mech. 118 (2022), 103250.
[12] Jr. J.C. Newman, I.S. Raju, Stress intensity factor equations for cracks in three dimensional finite bodies subjected to tension and bending loads. In: Computational Methods in the Mechanics of Fracture (Ed. S N Atluri), 1986, 312-334.
[13] Jr. J.C. Newman, Stress Intensity factor equations for very deep corner cracks at a circular hole in a plate. AIAA/ASCE/AHS/ASC Structures, Structural Dynamics and Materials Conference 2018: 1471.
[14] S.A. Fawaz, B. Andersson, Accurate stress intensity factor solutions for corner cracks at a hole, Engng. Fract. Mech. 71(9-10) (2004) 1235-1254.
[15] R.S. Barsoum, On the use of isoparametric finite elements in linear fracture mechanics, Int. J. Numer. Methods. Eng. 10(1) (1976) 25-37.
[16] Franc3D Reference Manual, 8.0. New York: Fracture Analysis Consultants, Ins. 2021. (www.fracanalysis.com)
[17] R.C. McClung, Y.D. Lee, J.W. Cardinal, Y. Guo, The pursuit of K: Reflections on the current state-of-the-art in stress intensity factor solutions for practical aerospace applications. 27th ICAF 2013; 1-18.
[18] H.F. Bueckner, Novel principle for the computation of stress intensity factors, Z Angew. Math. Mech. 50(9) (1970) 529-546.
[19] J.R. Rice, Some remarks on elastic crack-tip stress fields, Int. J. Solids. Struct. 8(6) (1972) 751-758.
[20] X.R. Wu, A.J. Carlsson, Weight Functions and Stress Intensity Factor Solutions. Pergamon Press, Oxford, UK. 1991.
[21] X.R. Wu, A review and verification of analytical weight function methods in fracture mechanics, Fatigue. Fract. Engng. Mater. Struct. 42(9) (2019) 2017-2042.
[22] X.R. Wu, W. Xu, Weight function methods in fracture mechanics: Theory and Applications. Springer & CAPM; 2022.
[23] X.R. Wu, W. Xu, Weight function theory and applications for crack analysis: a review and outlook (in Chinese). Advances in Mechanics, in press, 2022. https://doi.org/10.6052/1000-0992-

21-060
[24] M.H. Aliabadi, Numerical and Computational Methods, in Comprehensive Structural Integrity, 2003
[25] T. Fett, Direct determination of weight functions from reference loading cases and geometrical conditions, Eng. Fract. Mech. 42 (1992) 435-444.
[26] I.V. Orynyak, M.V. Borodii, V.M. Torop, Approximate construction of a weight function for quarter-elliptical, semi-elliptical and elliptical cracks subjected to normal stresses, Eng. Fract. Mech. 49 (1994) 143–151
[27] X, Wang, G, Glinka, Determination of approximate point load weight functions for embedded elliptical cracks, Int. J. Fatigue. 31 (2009) 1816-1827.
[28] T. Fett, D. Munz, Stress intensity factors and weight functions. Southampton, UK: Computational Mechanics Publications;1997.
[29] Z.Y. Jin, X. Wang, Point load weight functions for semi-elliptical cracks in finite thickness plate, J ASTM Int 9 (2012), 103962.
[30] R. Ghajar, H.S. Googarchin, General point load weight function for semi-elliptical crack in finite thickness plates, Engng. Fract. Mech. 109 (2013) 33-44.
[31] W. Guo, J.Q. Zhang, W.L. Guo, Two-dimensional weight function of stress intensity factors for corner cracks emanating from a circular hole, Engng. Fract. Mech. 252 (2021) 107821.
[32] W. Zhao, X.R. Wu, M.G. Yan, Weight function method for three dimensional crack problems—I. Basic formulation and application to an embedded elliptical crack in finite plates, Engng Fract Mech 34(3) (1989) 593-607.
[33] W. Zhao, X.R. Wu, M.G. Yan, Weight function method for three dimensional crack problems—II. Application to surface cracks at a hole in finite thickness plates under stress gradients, Engng Fract Mech 34(3) (1989) 609-624.
[34] W.T. Fujimoto, Determination of crack growth and fracture toughness parameters for surface flaws emanating from fastener holes. AIAA/ASME/SAE 17th Structures, Structural Dynamics, and Materials Conference, King of Prussia, Pa, 1976; 522-531.
[35] W. Zhao, Jr. J.C. Newman, M.A. Sutton, X.R. Wu, K.N, Shivakumar. Stress intensity factors for corner cracks at a hole by a 3-D weight function method with stresses from the finite element method, Fatigue. Fract. Engng. Mater. Struct. 20(9) (1997) 1255-1267.
[36] W. Zhao, Jr. J.C. Newman, M.A. Sutton, K.N. Shivakumar, X.R. Wu, Stress intensity factors for surface cracks at a hole by a three-dimensional weight function method with stresses from the finite element method. Fatigue Fract Engng Mater Struct. 21(2) (1998) 229-239.
[37] W. Zhao, Jr. J.C. Newman, M.A. Sutton, X.R. Wu, K.N. Shivakumar, Analysis of corner cracks at hole by a 3-D weight function method with stresses from finite element method. NASA TM-110144 1995.
[38] W. Zhao, Jr. J.C. Newman, M.A. Sutton, K.N. Shivakumar, X.R. Wu, Analysis of surface cracks at hole by 3-D weight function method with stresses from finite element method. NASA TM-110145 1995.
[39] X.R. Wu, Analytical wide-range weight functions for various finite cracked bodies, Eng. Anal. Bound. Elem. 9 (1992) 307-322.
[40] X.C. Zhao, X.R. Wu, D.H. Tong, Weight functions and stress intensity factors for pin-loaded single-edge notch bend specimen, Fatigue. Fract. Engng. Mater. Struct, 38 (2015) 1519-1528.
[41] X.C. Zhao, X.R. Wu, Jr. J.C. Newman, D.H. Tong, Stress intensity factors for surface cracks in single-edge notch bend specimen by a three-dimensional weight function method, Fatigue. Fract. Engng. Mater. Struct. 39 (2016) 1407-1418.
[42] J.G. Bakuckas, Comparison of boundary correction factor solutions for two symmetric cracks in a straight-shank hole, Engng. Fract. Mech 68 (2001) 1095-1106.
[43] B Zhang, W Xu, XR Wu. Weight function method and stress intensity factor for two unsymmetric through-thickness and quarter-elliptical corner cracks at circular hole, Engng. Fract. Mech. 264 (2022) 108361.
[44] B Zhang, W Xu, XR Wu. Three-dimensional weight function analyses and stress intensity factors for two unsymmetric surface cracks and surface-corner cracks at a circular hole. Theor Appl Fract Mech (2022): 103607.
[45] W Xu, B Zhang, XR Wu, Three-dimensional weight function analyses and stress intensity factors

for two eccentric and asymmetric surface cracks and surface-corner cracks at a circular hole, Engng. Fract. Mech. 277 (2023) 108972.

[46] Lv F, Zhou CY, Cheng RJ, Miao XT, He XH. A numerical analysis based on M-integral about the interaction of parallel surface cracks in an infinite plate. Theor Appl Fract Mech 2018; 96: 370-379.